

# ANALYSIS OF HIGH FIELD NON-LINEAR LOSSES ON SRF SURFACES DUE TO SPECIFIC TOPOGRAPHIC ROUGHNESS\*

Chen Xu<sup>#</sup> and Michael J. Kelley, The College of William and Mary, Williamsburg, VA 23187 USA  
Charles E. Reece, TJNAF, Newport News, VA 23606 USA

## Abstract

The high-field performance of SRF cavities will eventually be limited by the realization of fundamental material limits, whether it is  $H_{cl}$  or  $H_{sh}$ , or some derivative thereof, at which the superconductivity is lost. Before reaching this fundamental field limit at the macro level, it must be encountered at localized, perhaps microscopic, sites of field enhancement due to local topography. If such sites are small enough, they may produce thermally stabilized normal-conducting regions which contribute non-linear losses when viewed from the macro resonant field perspective, and thus produce degradation in  $Q_0$ . We have undertaken a calculation of local surface magnetic field enhancement from specific fine topographic structure by conformal mapping method and numerically. A solution of the resulting normal conducting volume has been derived and the corresponding RF Ohmic loss simulated.

## INTRODUCTION

It has been suspected that surface roughness can play a role in middle Q field slope and high Q drop in niobium superconducting radio frequency resonators. In fact, the Q decreasing phenomenon is a reflection of increasing surface resistance. [1]

Several models attempt to explain the Q slope/drop, some of them are promising, whereas, some contradict the further experiments. Even though it is a type II superconductor, niobium has Ginzburg-Landau factor around 1 which is on the boundary between first and second kind superconductors. Thus, in this report, we only consider Nb is a type I superconductor which has superheat magnetic critical field  $H_c$ . This  $H_c$  is temperature dependent. On the other hand, it is known, in some fine grain niobium cavities testing, that rough BCP surfaces are likely to exceed local magnetic or temperature transition values, thus more tendency to initiate quenching than smoother surface, such as EP or CBP surfaces. Statistically, engineering BCP surface has lower RMS height values ( $R_q$ ) and RMS slope values ( $R_{dq}$ ) than practical EP surfaces with the same characterizing surface area. In another sense, BCP treated surfaces, compared with EP surfaces, have more fluctuation of height and greater density of sharp features. Those high and sharp features might be potential ignition spots for magnetic normalization. To study the spread of normal zone in thermal equilibrium state, consideration of both electromagnetism and temperature are needed to model accurate RF losses.

\*Work supported by Jefferson Science Associates.

<sup>#</sup>xuchen@jlab.org

## SIMULATION

### Electromagnetism

Magnetic field enhancements from the geometry of sharp features can increase local surface magnetic field greater than the magnetic critical field. Within a given macroscopic surface area, the excited external magnetic field is homogenous and uniform. The local geometry magnetic field enhancement (LGMFE) will define where and at which field on the surface begins to lose superconductivity. Correct calculation is needed to determine effective surface resistance in order to conduct heat flow analysis. Temperature map will be calculated to determine the local superheat transition field. This feedback will increase normal zone area, until iteration reaches a new balance.

The algorithm to determine this phase transform front is to iterate and moving the calculation boundary to satisfy the known boundary condition. This boundary condition is the parallel H equals to  $H_{sh}$ . One can start with an actual surface with a given magnetic potential difference and calculate surface H field in the vacuum and local surface. If local surface field is greater than  $H_{sh}$  at one location, this suggests that materials under this location already lost superconductivity. Usually, this is because this location has sharp angle. After reducing this local point's height a certain small amount, calculate the field again until field on this location is equal (or smaller) than  $H_{sh}$ . The iteration is demonstrated in Fig. 1.

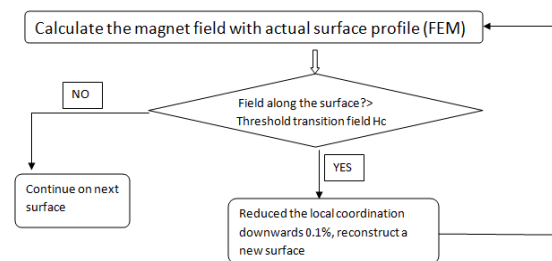


Figure 1: Flow chart to calculate E/M field configuration.

In order to increase from 0oe to 2000oe, magnetic scalar potential difference will be assigned as

$$H \text{ Magnetic field (A / m)} =$$

$$\frac{\Phi \text{ Magnetic scalar potential difference (A)}}{\text{Lateral length} (\mu\text{m})} \quad (1)$$

The magnetic scalar potential are added on boundaries 1 and 3, while on boundaries 2 and 4 is applied Perfect Electric Wall Condition (PEC) in Fig. 2.

In Fig. 2, H field is calculated with typical BCP surface, and boundaries are labelled with numbers [2]. The vertical contours are equal magnetic scalar potential

lines, while the horizontal contours are magnetic field flux direction.

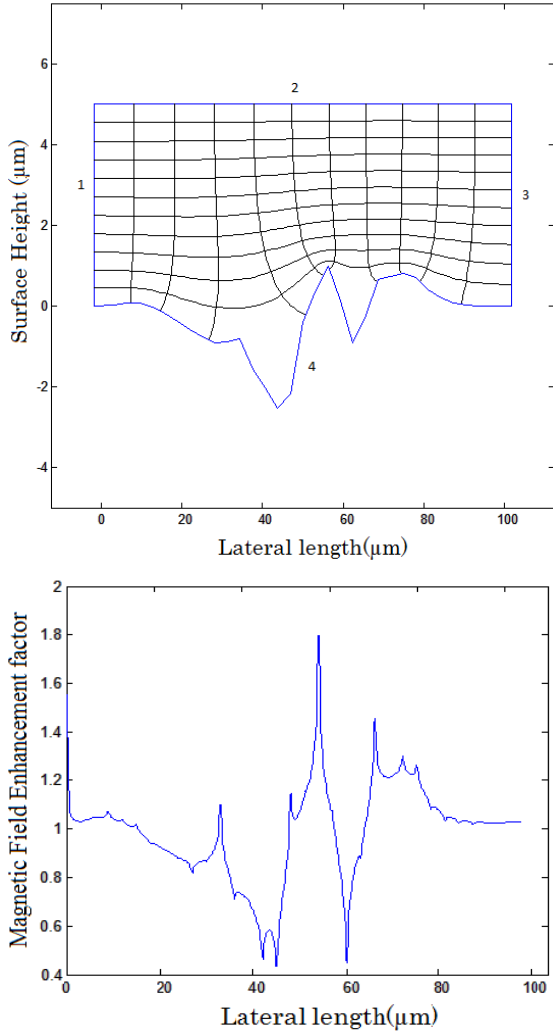


Figure 2: The Local Geometric Magnetic Field Enhancement factor (LGMFE) map along surface contour 4.

With applied potential difference as in Eq. 1, the NC/SC phase front is illustrated in Fig. 3. One can see how this stable interface moves inwards to bulk. Note that the interface is moving along with RF cycles. Therefore, the blue lines are the deepest boundaries that normal zone can reach. This interface movement should be carefully considered when calculating RF loss.

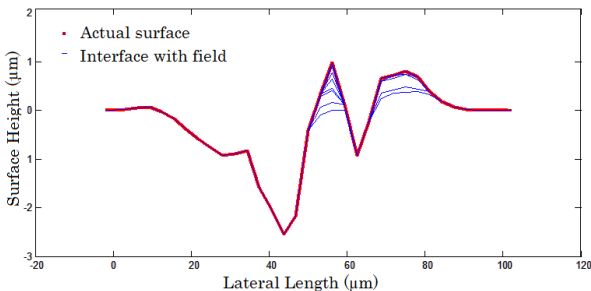


Figure 3: Normal conducting phase fronts are calculated from excited fields.

In Fig. 3, one can see that at low field, there is no normal zone because local field is weaker than Hsh. Since the highest LGMFE is around 2 in this example and Hsh is around 220mT, normal zone is expected to initiate at background H around 90mT. Such NC/SC interface will be input for RF loss calculation to obtain temperature map.

Temperature Simulation

Another critical point is the methods to obtain heat source in terms of RF power loss in this heat equation. Note, the conventional method that  $P = \int \frac{1}{2} R_s \cdot H^2 ds$  is not applicable in our study, because our assumption is the normal zone depth is smaller than normal skin depth. Then the heat should be calculated from volume integration of electric field with electric conductivity in the normal zone.

$$P = \int_{\Omega} \frac{1}{2} \times \sigma \times E^2 dV, \quad \Omega \text{ is normal zone}$$

We also simply presume E has only component normal to paper plane. Power is calculated in form of discrete power density on each element as an input vector for thermal simulation. Compared to RF loss in normal zone, the RF loss from superconducting zone is so trivial that it's neglected in this model despite its high temperature, because superconducting zone has comparably lower EM field and conductivity.

To obtain an accurate temperature map within the cavity wall, one needs to accommodate the temperature dependent thermal conductivity locally. This simulation calls for an iteration to reach temperature convergence. In each iteration, a new thermal conductivity map and Kapitza conductivity is reassigned, and iteration halts when temperature converges. The flow chart is provided in Fig. 4.

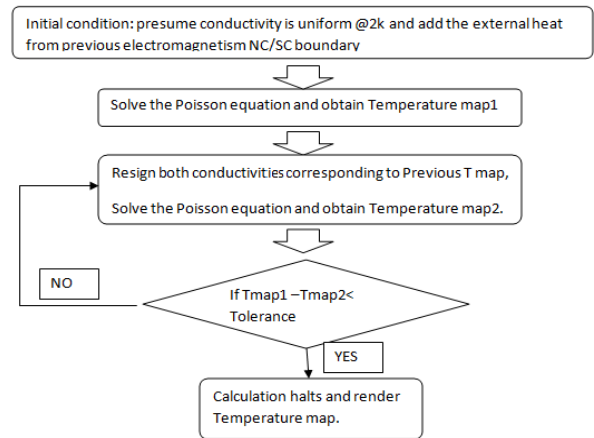


Figure 4: The flow chart of thermal equation simulation. With the electromagnetism output described in Fig. 4, one can calculate the temperature map across the cavity wall as demonstrated in figure below.

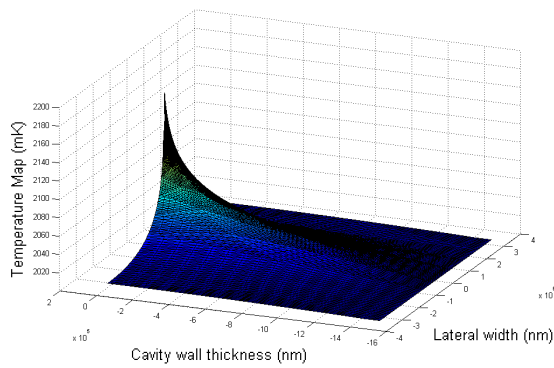


Figure 5: Temperature maps are calculated from magnetic scalar potentials on selective field 216mT.

From Fig. 5, one can see temperature increase at a hotspot. The heat affected zone can be as large as cm level. Even at 16A scalar potential which equals to 200mT, the highest temperature is not reaching 9.2K which is the Nb transition temperature. Thus, it is reasonable to claim that thermo-magnet quench is not happening on this surface at 120mT. However, the peak temperature near surface is reaching 2.2K at 220mT.

*Electromagnetism and Thermal ‘Big’ Iteration*

The superheat critical field of Nb is also dependent on temperature. The temperature on surface is calculated in Fig. 5. Thus we need to introduce thermal feedback model on H<sub>sh</sub> dependency and generate a big iteration on both simulation in section 2.1 and 2.2. A new SC/NC boundary is converged and given numerically. This big iteration flow chart is given in Fig. 6.

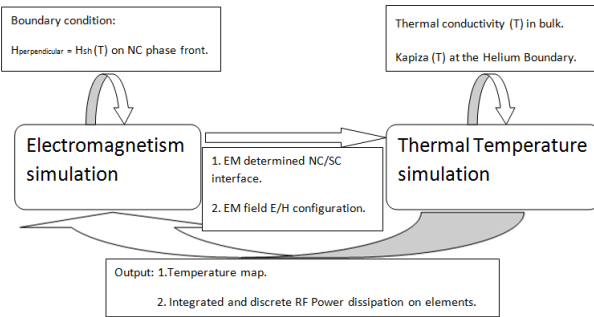


Figure 6: Flow chart of electromagnetism and temperature simulations.

In Fig. 6, the flow chart shows a big iteration with two small iterations. The big iteration is correction iteration. Fortunately, H<sub>sh</sub> has a steady trend at low field, thus this correction is minor.

The RF loss is calculated from increased external field. Fig. 7 gives the relation of RF loss and external field.

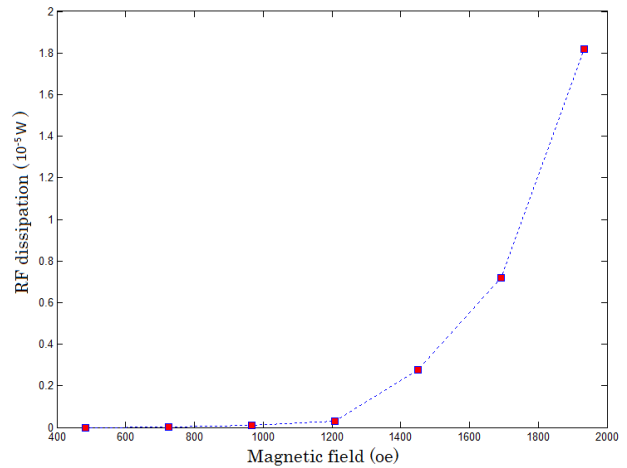


Figure 7: The integrated RF loss vs external magnetic field.

**DISCUSSION**

If heat flux is less condensed on one point but diluted into high density but weak heat source. Surface roughness RF power loss is applicable to this situation. Both situations are demonstrated and compared in Fig. 8.

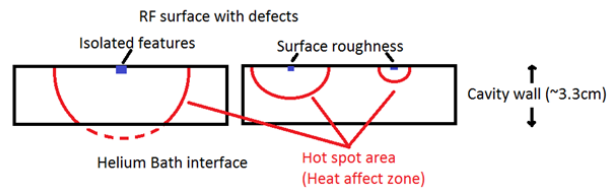


Figure 8: ‘Hotspot’ comparison between isolated and homogeneous surface features. The blue areas are geometric defects, while red circle suggests the ‘heat affected zone’.

**CONCLUSION**

An initial electromagnetism and thermal simulation has been conducted to obtain a normal and superconductivity conductor phase front for perfect topography of high field. This interface determines normal zone volume which contributes increasing non linear RF loss. Normal zone initiates its expanding based on local field geometric enhancement factor. With certain electromagnetic field applied, a thermal equilibrium is reached. More accurate normal zone phase front is obtained with critical field temperature dependency. Normal zone on the surface expands nonlinearly with increasing external magnetic field. Such nonlinearity can be represented in form of non-linear effective surface resistance at high field. A RF power loss contribution from topography can be calculated from this model and will be the subject of future works.

**REFERENCES**

[1] J. Knobloch. Proceeding of SRF 99, Santa Fe USA.  
 [2] Chen Xu et al. Phys. Rev.ST – AB. 14, (2011) pp.123501.

**ACKNOWLEDGMENT**

Authored by Jefferson Science Associates, LLC under U.S. DOE Contract No. DE-AC05-06OR23177. The U.S. Government retains a non-exclusive, paid-up, irrevocable, world-wide license to publish or reproduce this manuscript for U.S. Government purposes.

Copyright © 2012 by IEEE – cc Creative Commons Attribution 3.0 (CC BY 3.0) — cc Creative Commons Attribution 3.0 (CC BY 3.0)